

Joint Transmission Scheme and Coded Content Placement in Cluster-centric UAV-aided Cellular Networks

Zohreh HajiAkhondi-Meybodi, *Student Member, IEEE*, Arash Mohammadi, *Senior Member, IEEE*, Jamshid Abouei, *Senior Member, IEEE*, Ming Hou, *Senior Member, IEEE*

Abstract—Recently, as a consequence of the COVID-19 pandemic, dependence on telecommunication for remote learning/working and telemedicine has significantly increased. In this context, preserving high Quality of Service (QoS) and maintaining low latency communication are of paramount importance. Development of an Unmanned Aerial Vehicles (UAV)-aided heterogeneous cellular network is a promising solution to satisfy the aforementioned requirements. Although an integrated UAV-aided and cluster-centric cellular network can enhance connectivity and provide improved QoS, there are key challenges ahead for its efficient implementation. On the one hand, it is challenging to optimally increase content diversity in caching nodes to mitigate the network's traffic over the backhaul. On the other hand is the challenge of attenuated UAVs' signal in indoor environments, which increases users' access delay and UAVs' energy consumption. To address the aforementioned challenges, we incorporate UAVs, as mobile caching nodes, together with Femto Access points (FAPs) to increase the network's coverage in both indoor and outdoor environments. Referred to as the Cluster-centric and Coded UAV-aided Femtocaching (CCUF) framework, a two-phase clustering framework is proposed for optimal FAPs' formation and UAVs' deployment. The proposed CCUF implementation leads to an increase in the cache diversity, a reduction in the users' access delay, especially in indoor environments, and significant reduction in UAVs' energy consumption. To mitigate the inter-cell interference in edge areas, the Coordinated Multi-Point (CoMP) approach is integrated within the CCUF framework. In contrary to existing works, we analytically compute the optimal number of FAPs in each cluster to increase the cache-hit probability of coded content placement. Furthermore, the optimal number of coded contents to be stored in each caching node is computed to increase the cache-hit-ratio, Signal-to-Interference-plus-Noise Ratio (SINR), and cache diversity and decrease the users' access delay and cache redundancy for different content popularity profiles.

Index Terms—Cluster-centric, Coded Femtocaching, Coordinated Multi-Point (CoMP), Unmanned Aerial Vehicles (UAVs), Users' Access Delay.

Z. HajiAkhondi-Meybodi is with Electrical and Computer Engineering (ECE), Concordia University, Montreal, Canada. (E-mail: z_hajiak@encs.concordia.ca). A. Mohammadi (corresponding author) is with Concordia Institute of Information Systems Engineering (CIISE), Concordia University, Montreal, Canada. (P: +1 (514) 848-2424 ext. 2712 F: +1 (514) 848-3171, E-mail: arash.mohammadi@concordia.ca). J. Abouei was with the Department of Electrical, Computer and Biomedical Engineering, Ryerson University, Toronto, ON M5B 2K3, Canada. He is now with the Department of Electrical Engineering, Yazd University, Yazd 89195-741, Iran (E-mail: abouei@yazd.ac.ir). M. Hou is with Defence Research and Development Canada (DRDC), Ottawa, Toronto, ON, M2K 3C9, Canada. (E-mail: ming.hou@drdc-rddc.gc.ca).

This Project was partially supported by the Department of National Defence's Innovation for Defence Excellence and Security (IDEaS) program, Canada.

I. INTRODUCTION

As a consequence of the COVID-19 pandemic, dependence on telemedicine and remote learning/working has significantly increased due to the exponential rise in the demand for in-home care, remote working, schooling and remote reporting [1]. Within this context, to preserve real-time quality and integrity of large-sized multimedia data and provide high Quality of Service (QoS), it is of paramount importance to develop advanced heterogeneous networking solutions [2]. In this regard, caching has emerged as a promising solution to maintain low latency communication and mitigate the network's traffic over the backhaul. This, in turn, improves the QoS by storing the most popular multimedia contents close to the end-users [3], [4]. Recently, Unmanned Aerial Vehicle (UAV)-based caching has gained significant attention from both industry and academia [5]–[8], due to its high mobility, low cost and easy deployment characteristics. Although the enhanced connectivity that comes by using UAVs will improve the QoS in outdoor areas, there are key challenges ahead in indoor environments due to attenuation of the received signal [9]. To address this issue and in line with advancements of 5G networks, the paper focuses on coupling UAVs as aerial caching nodes with Femto Access Points (FAPs) [10], equipped with storage. The ultimate goal is to increase the caching network's QoS and its coverage in a heterogeneous environment (i.e., integrated indoor and outdoor settings).

Literature Review: There are several challenges in development of UAV-aided caching networks, including placement optimization [11], [12]; trajectory design [13], [14]; resource allocation [15], [16], and; energy consumption management [17], [18]. Existing works [11]–[22] mainly focus on the deployment of UAVs in outdoor environments. There are several benefits that come with utilization of UAVs as aerial caching nodes such as high probability of establishing Line-of-Sight (LoS) links between UAVs and ground users. Such benefits, however, result in several critical challenges especially in indoor environments due to signal attenuation [23]. This level of obfuscation in an integrated indoor and outdoor environment can be settled by design of UAV-aided cellular networks [24].

One of the main challenges in UAV-aided cellular networks is to optimally assign caching nodes (UAVs or FAPs) to ground users to efficiently serve their requests [25], [26]. There are several QoS and Quality of Experience (QoE) metrics that

can be considered as the decision criteria for Access Point (AP) selection, including users' latency; traffic load and energy consumption of APs; users' link quality; handover rate, and; Signal-to-Interference-plus-Noise Ratio (SINR). For instance, Athukoralage *et al.* [25] considered an AP selection framework, where ground users are supported by UAV or WiFi APs. In this work, the users' link quality is utilized to balance the load between UAVs and WiFi APs. Zhu *et al.* [26] proposed a game theory-based AP selection scheme, where probability of packet collision is used to select the optimal AP among all possible UAVs and Base Stations (BSs). Considering the fact that users' mobility is one of the inherent features of current ultra-dense wireless networks, movement characteristics, such as speed of ground users, must be considered as a decision criteria for connection scheduling. To date, limited research has been performed on UAV-aided cellular networks to address the aforementioned problem of connection scheduling between FAPs and UAVs in a heterogeneous environment considering the speed of users' movement. The paper addresses this gap.

In UAV-aided cellular networks, the main objective is to bring multimedia data closer to ground users and simultaneously improve users' QoS and network's QoE. If the requested content can be found in the storage of one of the available caching nodes, this request would be served directly and cache-hit occurs; otherwise, it is known as a cache-miss. Due to the large size of multimedia contents, however, it is not feasible to store all contents in the storage of caching nodes. To overcome this problem, coded caching strategies, such as Linear Random Fountain Code (LRFC) [27], and Maximum Distance Separable (MDS) [28] coding schemes have received remarkable attention lately. In such coded caching strategies, only specific segments of the most popular multimedia contents are stored in the caching nodes. Storing coded popular contents increases the overall content diversity. In coded femtocaching frameworks, however, most early works such as Reference [29] consider *homogeneous* networks, where the same segments of the most popular multimedia contents are stored in different caching nodes. To overcome this issue, the main focus of recent researchers has been shifted to *heterogeneous* networks with an emphasis on the mobility of ground users and overlapped caching nodes [30]. Toward this goal, Chen *et al.* [31] proposed a cluster-centric small cell network, where popular contents are classified into two different categories, i.e., the Most Popular Contents (MPCs), and the Large Popular Contents (LPCs). While MPCs are completely stored in the storage of all Small Base Stations (SBSs), distinct segments of LPCs are cached in different SBSs.

Cluster-centric cellular networks provide several benefits, such as increased content/cache diversity, which in turn leads to remarkable growth in the number of requests managed by the caching nodes. However, this comes with the cost of experiencing inter-cell interference especially for cell-edge users. To tackle this issue, Chen *et al.* [31] employed the Coordinated Multi-Point (CoMP) approach to mitigate the inter-cell interference and improve the throughput of ground users located in the cell-edges. Reference [31] developed two transmission schemes, namely Joint Transmission (JT) and Parallel Transmission (PT), which are selected based on

the popularity of the requested content. Alternatively, Lin *et al.* [32] proposed a cluster-centric cellular network applying the CoMP technique based on the users' location, where cell-core and cell-edge users are served through Single Transmission (ST) and JT, respectively. Despite all the researches on the cluster-centric cellular networks, there is no framework to determine how different segments can be cached to increase the data availability in a UAV-aided cluster-centric cellular network integrated by the CoMP technology. The paper also addresses this gap.

Contribution: In this paper, we consider an integrated UAV-aided and cluster-centric cellular network to serve ground users positioned in both indoor and outdoor environments. Our first objective is to increase the content diversity that can be accessed via the caching nodes. The second goal is to assign ground users the best caching nodes to improve the achievable QoS in terms of the users' access delay and decrease the energy consumption of UAVs. To achieve the above-mentioned objectives, the paper proposes a novel Cluster-centric and Coded UAV-aided Femtocaching (CCUF) framework, in which the caching node and the transmission scheme are jointly determined based on the movement features of ground users and the CoMP technology. Moreover, to increase content diversity, an analytical solution is derived to allocate distinct segments of the multimedia contents in different neighboring FAPs. In summary, the paper makes the following key contributions:

- Indoor penetration loss and deep shadow fading caused by building walls significantly attenuate the UAV's signals in indoor environments degradation the network's QoS. To tackle this issue, we consider two different indoor and outdoor caching service scenarios for the proposed CCUF framework. More precisely, the indoor area is covered by FAPs, equipped with extra storage. The outdoor, however, is supported by coupled UAVs and FAPs depending on the movement speed of ground users.
- Due to the limited storage of caching nodes, the most popular multimedia contents are determined based on the solution of a formulated optimization problem. Consequently, multimedia contents are fragmented into the same size segments based on the Fountain codes.
- With the focus on a dynamic UAV-based femtocaching network, storing distinct contents in neighboring FAPs increases the resource availability. In contrary to existing coded caching approaches [31], [32] that lack utilization of placement strategies to allocate segments of video contents to different caching nodes, the proposed CCUF scheme determines a solution to store different segments of contents in neighboring FAPs. Toward this goal, we consider a cluster-centric cellular network, where multimedia contents are classified into three categories, including popular, mediocre, and non-popular contents. While the popular contents are stored completely, distinct segments of mediocre ones are determined according to the proposed framework to be stored in the storage of neighboring FAPs. In this paper, we determine the best number of coded and uncoded contents in each caching node to increase the cache-hit-ratio, SINR, and cache

diversity while decreasing users' access delay and cache redundancy for different content popularity profiles.

- To simulate a real wireless network, we consider mobile ground users, where the Angle of Arrival (AoA) localization technique is utilized to estimate the initial location of ground users. Then, the mobility pattern is presented by the Difference Correlated Random Walk (DCRW) model. To access a large amount of contents during movement of ground users, two scenarios are proposed: (i) The whole network is partitioned into sub-networks called inter-clusters. All FAPs in the same inter-cluster save different parts of mediocre contents, while the cached contents of different inter-clusters are the same. In this case, it can be shown that ground users can acquire more segments during their movements, and; (ii) To increase the resource availability, the outdoor environment is partitioned into intra-clusters via a K-means clustering algorithm, each covered by a UAV.
- To mitigate the inter-cell interference in inter-clusters and provide more efficient service for edge users, the CoMP technique is utilized, including ST and JT schemes. Note that the transmission type depends on both the popularity of contents and the position of the ground user in the cell.

The effectiveness of the proposed CCUF framework is evaluated through simulation studies in both indoor and outdoor environments in terms of cache-hit-ratio, users' access delay, SINR, cache diversity, cache redundancy, and energy consumption of UAVs. According to the simulation results, we investigate the best number of coded contents in each caching node to increase the cache-hit-ratio, SINR, and cache diversity and decrease users' access delay and cache redundancy for different content popularity profiles. Moreover, we investigate the effects of the UAV-aided femtocaching network on the users' access delay and energy consumption of UAVs in both indoor and outdoor environments.

The remainder of the paper is organized as follows: In Section II, the network's model is described and the main assumptions required for the implementation of the proposed framework are introduced. Section III presents the proposed CCUF scheme. Simulation results are presented in Section IV. Finally, Section V concludes the paper.

II. SYSTEM MODEL AND PROBLEM DESCRIPTION

We consider a UAV-aided cellular network in a residential area that supports both indoor and outdoor environments. There exist N_f number of FAPs, denoted by f_i , for $(1 \leq i \leq N_f)$, each with the cache size of C_f and transmission range of R_f . There are also N_u number of UAVs, denoted by u_k , for $(1 \leq k \leq N_u)$, with equal transmission range of R_u . The transmission range of each FAP is significantly less than that of a UAV. As it can be seen from Fig. 1, $N_s < N_f$ number of FAPs in a neighborhood form a cluster, referred to as the inter-cluster. Similarly, N_{ic} number of FAPs in the outdoor environment form an intra-cluster covered by a UAV. There are N_g number of ground users, denoted by GU_j , for $(1 \leq j \leq N_g)$, that move through the network with different velocities. $v_j(t)$ denotes the speed of the ground user GU_j at

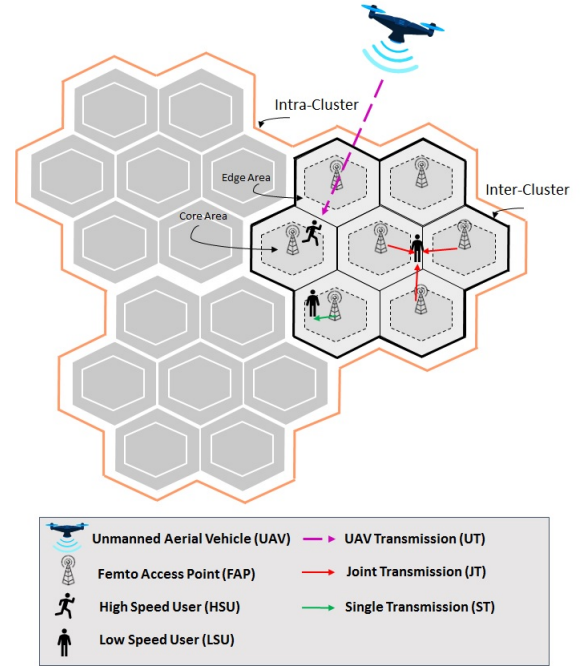


Fig. 1: A typical structure of the proposed UAV-aided cellular network.

time slot t . In this work, FAP f_i , for $(1 \leq i \leq N_f)$, operates in an open access mode, i.e., it can serve any ground user GU_j , for $(1 \leq j \leq N_g)$, located in its transmission range. The FAPs within each inter-cluster use the CoMP transmission approach (supporting ST and JT schemes) to mitigate the inter-cell interference in edge areas and manage ground users' requests. To completely download a requested content, a finite time T is required. For ease of exposition, the time T is discretized into N_s time slots with time interval δ_t , i.e., $T = N_s \delta_t$. In what follows, we present users' mobility pattern, the content popularity profile, and transmission schemes utilized to develop the proposed CCUF.

A. Users' Mobility Pattern

In the proposed CCUF framework, estimated location of GUs is required to determine the transmission scheme and select an appropriate caching node to manage the request. Capitalizing on the reliability and efficiency of the AoA localization technique [33], [34], it is utilized to identify the initial location of GUs as follows

$$x_j(0) = \frac{d_{n,i} \tan \theta_{i,j}}{\tan \theta_{i,j} - \tan \theta_{n,j}}, \quad (1)$$

$$y_j(0) = \frac{d_{n,i} \tan \theta_{n,j} \tan \theta_{i,j}}{\tan \theta_{i,j} - \tan \theta_{n,j}}, \quad (2)$$

where $\mathbf{l}_j(0) = [x_j(0), y_j(0)]^T$ is the location of ground user GU_j at time $t = 0$. In addition, $d_{n,i}$ indicates the distance between the i^{th} and the n^{th} FAPs, assuming the positions of FAPs are known. Moreover, the angle between the line from the location of the ground user GU_j to FAP f_i and X-axis is denoted by $\theta_{i,j}$ [34].

Given the initial location of ground users, we use the Difference Correlated Random Walk (DCRW) [35] to model

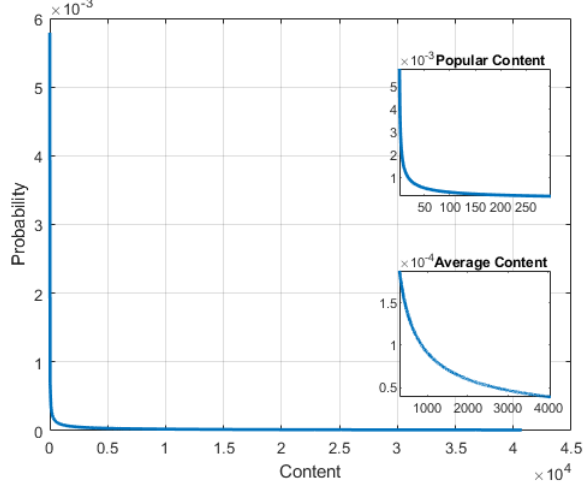


Fig. 2: Zipf distribution.

their movement patterns. In this regard, the location of GU_j at time slot t , denoted by $\mathbf{l}_j(t)$, is given by

$$\mathbf{l}_j(t) = \mathbf{l}_j(t-1) + \mathbf{v}_j(t-1)\Delta t, \quad (3)$$

where Δt is the time interval between two consecutive estimated locations, and $\mathbf{v}_j(t) = [v_j^{(x)}(t), v_j^{(y)}(t)]^T$ denotes the user's velocity, obtained as follows [35]

$$d\mathbf{v}_j(t) = - \begin{pmatrix} -\log \varsigma_1 & \theta \\ -\theta & -\log \varsigma_2 \end{pmatrix} (\mathbf{v}_j(t) - \boldsymbol{\mu})dt + \mathbf{J}d\mathbf{b}_t, \quad (4)$$

where ς_1 and ς_2 denote auto-correlation parameters in X -axis and Y -axis, respectively. Terms θ and $\boldsymbol{\mu}$ represent the mean turning angle and the mean velocity vector, respectively. Term \mathbf{J} represents the velocity shifts covariance, which is a (2×2) lower triangular matrix with positive diagonal components. Finally, \mathbf{b}_t , which is a (2×1) vector, determines the standard Brownian motion at time slot t .

B. Content Popularity Profile

When the ground user GU_j requests content c_l from a library of $\mathcal{C} = \{c_1, \dots, c_{N_c}\}$, in which N_c is the cardinality of multimedia data in the network, this request should be handled by one of the nearest FAPs or UAVs having some segments of c_l . Regarding the user's behavior pattern in multimedia services, the popularity of video contents is determined based on the Zipf distribution [36], where the probability of requesting l^{th} file, denoted by p_l , is calculated as

$$p_l = \frac{l^{-\gamma}}{\sum_{r=1}^{N_c} r^{-\gamma}}, \quad (5)$$

where γ represents the skewness of the file popularity. In the proposed CCUF framework, each content c_l is fragmented into N_s encoded segments, denoted by c_{ls} , for $(1 \leq s \leq N_s)$, which is the same as the number of FAPs in each inter-cluster. The ground user GU_j can download one segment in δ_t , which is equivalent to $1/N_s$ of a multimedia content. In other words, in each contact, user GU_j will leave the transmission area of the current FAP. For notational convenience, we assume that

$P[n] \equiv P(n\delta_t)$ denotes the probability of accessing a new segment in time slot n , with $n \in \{0, \dots, N_s\}$.

Without loss of generality and to be practical, we investigate the probability distribution of a real multimedia data set, i.e., the YouTube videos trending statistics, shown in Fig. 2. As it can be seen from Fig. 2, the probability distribution follows Zipf, i.e., a small part of the contents are requested with a high probability. The majority of contents are not popular, and some contents, are requested moderately. Consequently, in our cluster-centric UAV-aided cellular network, we classify multimedia contents into three categories, including popular, mediocre, and non-popular [31]. To improve content diversity, the storage capacity of FAPs, denoted by C_f , is divided into two spaces, where α portion of the storage is allocated to store complete popular contents, i.e., $1 \leq l \leq \lfloor \alpha C_f \rfloor$, where $l = 1$ indicates the most popular content. Additionally, $(1 - \alpha)$ portion of the cache is assigned to store different parts of the mediocre contents, where $\lfloor \alpha C_f \rfloor + 1 \leq l \leq N_s(C_f - \lfloor \alpha C_f \rfloor)$. The optimal value of α is obtained experimentally. The proposed model for identifying different segments to be cached in neighboring FAPs will be discussed later on in Section III.

C. Transmission Scheme

In this subsection, we will describe both the connection scheduling (serving by FAPs or UAVs) and the transmission scheme depending on the presence of the ground user in indoor or outdoor environments.

1) *Indoor Environment*: The transmitted signal by UAVs, propagating in residential areas, becomes weaker due to the penetration loss and shadow fading effects. Therefore, it is assumed that ground users positioned in indoor areas are only supported by FAPs. In the CoMP-integrated and cluster-centric cellular network and as it can be seen from Fig. 1, there are two regions in each inter-cluster, named cell-edge and cell-core, which are determined based on the SINR value to illustrate the quality of a wireless link. In such a case that the ground user GU_j is positioned in the vicinity of the FAP f_i , the SINR from f_i to GU_j , denoted by $\mathcal{S}_{i,j}$, is obtained as follows

$$\mathcal{S}_{i,j}(t) = \frac{P_i |\tilde{\mathcal{H}}_{i,j}(t)|^2}{I_{f-i}(t) + N_0}, \quad (6)$$

where P_i denotes the transmitted signal power of FAP f_i . $I_{f-i}(t)$ and N_0 represent the interference from other FAP-ground users, except for the corresponding f_i link, and the noise power related to the additive white Gaussian random variable, respectively. Moreover, the path loss and fading channel effect between FAP f_i and ground user GU_j at time slot t is denoted by $\tilde{\mathcal{H}}_{i,j}(t) = \frac{h_{i,j}(t)}{\sqrt{\mathcal{L}_{i,j}(t)}}$. In this case, $h_{i,j}(t)$ denotes a complex zero-mean Gaussian random variable with unit standard deviation and $\mathcal{L}_{i,j}(t)$ represents the path loss between FAP f_i and ground user GU_j at time slot t , obtained as follows

$$\mathcal{L}_{i,j}(t) = \mathcal{L}_0 + 10\eta \log(d_{i,j}(t)) + \chi_\sigma, \quad (7)$$

where η is the path loss exponent. Term χ_σ indicates the shadowing effect, which is a zero-mean Gaussian-distributed random variable with standard deviation σ . Additionally, $d_{k,j}(t)$

represents the Euclidean distance between FAP f_i and ground user GU_j at time slot t . Furthermore, $\mathcal{L}_0 = 20 \log \left(\frac{4\pi f_c d_0}{c} \right)$ is the path loss related to the reference distance d_0 where f_c and $c = 3 \times 10^8$ denote the carrier frequency and the light speed, respectively. Accordingly, the ground user GU_j is located at the cell-core of FAP f_i , if $\mathcal{S}_{i,j}(t) > \mathcal{S}_{th}$; otherwise, GU_j is located at the cell-edge, where \mathcal{S}_{th} is the SINR threshold.

The transmission scheme in the proposed CoMP-integrated and cluster-centric cellular network is determined based on two metrics; (i) The popularity of the requested content, described in Subsection II-B, and; (ii) The location of the ground user in the cell, i.e., cell-core or cell-edge. The following two different transmission schemes are utilized for development of the proposed CCUF framework:

- **Single Transmission (ST):** In this case, the requested file c_l , for $(1 \leq l \leq \lfloor \alpha C_f \rfloor)$, is popular content, and the ground user GU_j is located at the cell-core of FAP f_i , i.e., $\mathcal{S}_{i,j}(t) > \mathcal{S}_{th}$. It means that the content is completely cached into the storage of FAP f_i and the high-quality link can be established between FAP f_i and ground user GU_j . Consequently, this request is served only by the corresponding FAP f_i . Moreover, if the requested content, belongs to the mediocre category, i.e., $\lfloor \alpha C_f \rfloor + 1 \leq l \leq N_s(C_f - \lfloor \alpha C_f \rfloor)$, regardless of the location of the ground user, this request served according to the ST scheme.
- **Joint Transmission (JT):** In this transmission scheme, the requested file c_l is popular content, i.e., $1 \leq l \leq \lfloor \alpha C_f \rfloor$. Consequently, all FAPs have the same complete file. The ground user GU_j , however, is located at the cell-edge of FAP f_i , i.e., $\mathcal{S}_{i,j}(t) \leq \mathcal{S}_{th}$. Therefore, the link quality between FAP f_i and the ground user GU_j is not good enough. In order to improve the reliability of content delivery, the corresponding content will be jointly transmitted by several FAPs in its inter-cluster. As it can be seen from Fig. 1, neighboring FAPs in an inter-cluster collaboratively serve cell-edge ground users based on the JT scheme, which is shown by the red color.

2) *Outdoor Environment:* The wide transmission range of UAVs and the high probability of establishing LoS link provide several advantages, including the ability to manage the majority of ground users' requests, which leads to improved coverage in outdoor environments. Due to the limited battery life of UAVs, however, requests that are handled by UAVs should be controlled. For this reason, we consider a UAV-aided femtocaching network in the outdoor environment. Note that we also need to reduce the number of handovers, which can be frequently triggered by FAPs, if the ground user moves and leaves the current position rapidly. Toward this goal, ground users are classified based on their velocity into the following two groups:

- **Low Speed Users (LSUs):** If the speed of ground user GU_j , denoted by $v_j(t)$, is less than a predefined threshold v_{th} , this user can be managed by inter-clusters. Similar to the indoor environments, the transmission scheme is determined based on the content popularity profile and the ground user's location.

- **High Speed Users (HSUs):** In this case, the speed of ground user GU_j is equal or more than v_{th} . Therefore, this request should be served by a UAV that covers the corresponding intra-cluster.

This completes our discussion on users' mobility pattern, the content popularity profile, and transmission schemes. Next, we develop the CCUF framework.

III. THE CCUF FRAMEWORK

In conventional femtocaching schemes, it is commonly assumed that all caching nodes store the same most popular contents. This assumption is acceptable in static femtocaching models, in which users are stationary or move with a low velocity. With the focus on a dynamic femtocaching network, in which users can move based on the random walk model, storing distinct contents in neighboring FAPs leads to increasing the number of requests served by caching nodes. Despite recent researches on cluster-centric cellular networks, there is no framework to determine how different segments should be stored to increase content diversity. Toward this goal, we propose the CCUF framework, which is an efficient content placement strategy for the network model introduced in Section II. The most remarkable idea behind the CCUF strategy is to identify the most widely requested contents to maximize the cache-hit-ratio and minimize the users' access delay. Given the common content, an inter-cluster is formed by N_s number of adjacent FAPs, in which distinct segments of coded content are stored in the FAP's cache. Consequently, the number of requests served by caching nodes drastically increases without any growth of the storage of FAPs. Additionally, N_{ic} number of near FAPs as an intra-cluster is managed by one UAV to provide low-latency communication for outdoor ground users. The proposed CCUF framework is implemented based on the steps presented in the following subsections.

A. Optimal Content Caching for FAPs and UAVs

Identifying the optimal multimedia contents to be stored in the storage of caching nodes leads to a reduction in the users' latency. It is a commonly assumed [3], [29] that the total users' access delay is determined according to availability of the required content in the nearby caching nodes. Based on this assumption, in scenarios where the requested content can be served by caching nodes, the cache-hit occurs and the ground user will experience no delay; otherwise, the request is served by the main server resulting in a cache-miss. In this paper, we relax the above assumption and express the users' access delay as a function of the content popularity profile and the distance between the ground user and the target caching node. In the regard, we propose two optimization models for content placement in both FAPs and UAVs to minimize the users' latency. Toward this goal, first we describe the delay that ground users experience when served by FAPs and UAVs.

1) *UAVs' Content Placement:* In order to calculate the users' access delay through UAVs, first, we investigate the effect of distance between ground user GU_j and target UAV u_k . Serving requests via UAVs leads to establishing air-to-ground links from UAVs to ground users. Due to the obstacles

in outdoor environments, the transmitted signal from UAVs is attenuated. To be practical, we consider both LoS and Non-LoS (NLoS) path losses from UAV u_k to ground user GU_j at time slot t as follows [5]

$$\mathcal{L}_{k,j}^{(LoS)}(t) = \mathcal{L}_0 + 10\eta^{(LoS)} \log(d_{k,j}(t)) + \chi_\sigma^{(LoS)}, \quad (8)$$

$$\mathcal{L}_{k,j}^{(NLoS)}(t) = \mathcal{L}_0 + 10\eta^{(NLoS)} \log(d_{k,j}(t)) + \chi_\sigma^{(NLoS)}, \quad (9)$$

where $\mathcal{L}_0 = 20 \log \left(\frac{4\pi f_c d_0}{c} \right)$ denotes the reference path loss in distance d_0 , and $d_{k,j}(t)$ is the Euclidean distance between UAV u_k and the ground user GU_j at time slot t . In addition, $\eta^{(LoS)}$, $\eta^{(NLoS)}$, $\chi_\sigma^{(LoS)}$ and $\chi_\sigma^{(NLoS)}$ indicate the LoS and NLoS path loss exponents and the corresponding shadowing effects, respectively. Consequently, the average path loss, denoted by $\bar{\mathcal{L}}_{k,j}(t)$, is obtained as

$$\bar{\mathcal{L}}_{k,j}(t) = p_{k,j}^{(LoS)}(t) \mathcal{L}_{k,j}^{(LoS)}(t) + (1 - p_{k,j}^{(LoS)}(t)) \mathcal{L}_{k,j}^{(NLoS)}(t), \quad (10)$$

where $p_{k,j}^{(LoS)}(t)$ is the probability of establishing LoS link between UAV u_k and ground user GU_j at time slot t , obtained as [15]

$$p_{k,j}^{(LoS)}(t) = (1 + \vartheta \exp(-\zeta[\phi_{k,j}(t) - \vartheta]))^{-1}, \quad (11)$$

where ϑ and ζ are constant parameters, depending on the rural and urban areas. Moreover, $\phi_{k,j}(t) = \sin^{-1} \left(\frac{h_k}{d_{k,j}(t)} \right)$ is the elevation angle between UAV u_k and the ground user GU_j , and h_k is the UAV's altitude. Without loss of generality, altitude h_k is assumed to be a fixed value over hovering time. If the requested content cannot be found in the storage of UAVs, additional ground-to-air connection is required to provide UAVs with the requested content through the main server. Similarly, the average path loss of the main server-to-UAV u_k link is calculated as

$$\bar{\mathcal{L}}_{m,k}(t) = p_{m,k}^{(LoS)}(t) \mathcal{L}_{m,k}^{(LoS)}(t) + (1 - p_{m,k}^{(LoS)}(t)) \mathcal{L}_{m,k}^{(NLoS)}(t), \quad (12)$$

where $\mathcal{L}_{m,k}^{(LoS)}(t) = d_{m,k}^{-\varpi}(t)$ and $\mathcal{L}_{m,k}^{(NLoS)}(t) = \psi \mathcal{L}_{m,k}^{(LoS)}(t)$, in which $d_{m,k}(t)$ denotes the distance between the main server and UAV u_k . Furthermore, ϖ and ψ denote the LoS and NLoS path loss exponents, respectively [5].

As mentioned previously, another parameter that has a great impact on the users' access delay is the presence of the requested content in the caching node, depending on the content popularity profile. Therefore, the cache-hit and the cache-miss probability through serving by UAV u_k at time slot t , denoted by $p_u^{(h)}(t)$ and $p_u^{(m)}(t)$, respectively, are expressed as

$$p_u^{(h)}(t) = \sum_{l \in C_u} p_l(t) \leq 1, \quad (13)$$

$$p_u^{(m)}(t) = 1 - p_u^{(h)}(t), \quad (14)$$

where C_u denotes the cache size of UAV u_k , which is assumed to be the same for all UAVs. Consequently, the users' access delay through UAVs is expressed as

$$\mathcal{D}_u(t) = p_u^{(h)}(t) \mathcal{D}_u^{(h)}(t) + p_u^{(m)}(t) \mathcal{D}_u^{(m)}(t), \quad (15)$$

where $\mathcal{D}_u^{(h)}(t)$ and $\mathcal{D}_u^{(m)}(t)$ represent the cache-hit and the cache-miss delays, respectively, calculated as follows

$$\mathcal{D}_u^{(h)}(t) = \frac{L_c}{R_{k,j}} = L_c \log^{-1} \left(1 + \frac{P_k 10^{\bar{\mathcal{L}}_{k,j}(t)/10}}{I_k(t, \mathbf{u}_{-k}) + N_0} \right) \quad (16)$$

$$\mathcal{D}_u^{(m)}(t) = \underbrace{L_c \log^{-1} \left(1 + \frac{P_k 10^{\bar{\mathcal{L}}_{m,k}(t)/10}}{I_k(t, \mathbf{u}_{-k}) + N_0} \right)}_{\triangleq L_{MU}} + \underbrace{L_c \log^{-1} \left(1 + \frac{P_k 10^{\bar{\mathcal{L}}_{k,j}(t)/10}}{I_k(t, \mathbf{u}_{-k}) + N_0} \right)}_{\triangleq L_{UG}}, \quad (17)$$

where L_c and $R_{k,j}$ represent the file size of c_l and the transmission data rate from UAV u_k to GU_j . Furthermore, P_k and $I_k(t, \mathbf{u}_{-k})$ denote the transmission power of UAV u_k and the interference caused by other UAV-user links for the transmission link between u_k and GU_j , respectively. Note that when the cache-miss happens, the content should be first provided for the UAV by the main server. Therefore, L_{MU} and L_{UG} in Eq. (17) represent the users' access delay related to the main server-UAV and UAV-ground user links, respectively.

Given users' access delay through UAVs, the goal is to place contents in the storage of UAVs to minimize the users' access delay in Eq. (15). Due to the large coverage area of UAVs, it is not feasible to move through areas supported by different UAVs frequently. Therefore, we assume that contents are cached completely (either popular or mediocre ones). Toward this goal, the cached contents are selected as the solution of the following optimization problem to minimize the users' access delay:

$$\begin{aligned} \min_{\mathbf{x}_l} \quad & \sum_{l=1}^{N_c} \left(\sum_{j=1}^{N_g} (1 - p_l^{(j)}(t)) \mathcal{D}_u^{(j)}(t) \right) x_l \\ \text{s.t.} \quad & \mathbf{C1.} \quad x_l \in \{0, 1\}, \\ & \mathbf{C2.} \quad \sum_{l=1}^{N_c} x_l \leq C_u, \end{aligned} \quad (18)$$

where $p_l^{(j)}(t)$ denotes the probability of requesting content c_l by the ground user GU_j at time slot t , which is obtained according to the request history of ground users [3]. Furthermore, $\mathcal{D}_u^{(j)}(t)$ is the delay that the ground user GU_j may experience, which is calculated based on Eq. (15). In the constraint **C1**, x_l is an indicator variable, which is equal to 1 when content c_l exists in the cache of UAV u_k . Moreover, the constraint **C2** represents that the total contents cached in the storage of u_k should not exceed the storage capacity of UAV u_k .

2) *FAPs' Content Placement*: Serving requests by FAPs leads to a ground-to-ground connection type between FAPs and ground users. Similarly, the users' access delay through FAP connections is calculated as

$$\mathcal{D}_f(t) = p_k^{(h)}(t) \mathcal{D}_f^{(h)}(t) + p_k^{(m)}(t) \mathcal{D}_f^{(m)}(t), \quad (19)$$

where $\mathcal{D}_f^{(h)}(t)$, as the cache-hit delay, is expressed as

$$\mathcal{D}_f^{(h)}(t) = L_c \log^{-1} (1 + \mathcal{S}_{i,j}(t)), \quad (20)$$

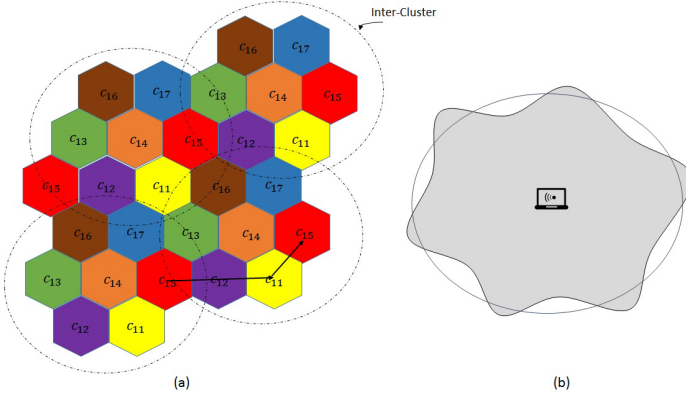


Fig. 3: (a) A typical hexagonal cellular network, where seven FAPs form an inter-cluster, (b) Real coverage area of FAPs in a practical model.

with $S_{i,j}(t)$ denoting the SINR from f_i to GU_j defined in Eq. (6). The optimal coded contents to be stored in the storage of FAPs are determined according to the solution of the following optimization problem:

$$\begin{aligned}
 \mathcal{F}(\mathbf{y}, \mathbf{z}) = & \min_{\mathbf{y}_l, \mathbf{z}_l} \sum_{l=1}^{\lfloor \alpha C_f \rfloor} \left(\sum_{j=1}^{N_g} (1 - p_l^{(j)}(t)) \mathcal{D}_f^{(j)}(t) \right) y_l \quad (21) \\
 & + \sum_{l=\lfloor \alpha C_f \rfloor + 1}^{N_s(C_f - \lfloor \alpha C_f \rfloor)} \left(\sum_{j=1}^{N_g} (1 - p_l^{(j)}(t)) \mathcal{D}_f^{(j)}(t) \right) z_l, \\
 \text{s.t.} \quad & \mathbf{C1.} \quad y_l, z_l \in \{0, 1\}, \\
 & \mathbf{C2.} \quad \sum_{l=1}^{\lfloor \alpha C_f \rfloor} y_l \leq \alpha C_f, \\
 & \mathbf{C3.} \quad \sum_{l=1}^{N_s(C_f - (1+N_s)\lfloor \alpha C_f \rfloor)} z_l \leq (1 - \alpha) N_s C_f,
 \end{aligned}$$

where $\mathcal{F}(\mathbf{y}, \mathbf{z})$ is the cost function associated with users' access delay, experienced by serving the request through FAPs. By assuming that $N_p = \lfloor \alpha C_f \rfloor$ and $N_a = N_s(C_f - \lfloor \alpha C_f \rfloor)$ are the cardinality of popular and mediocre contents, respectively, $\mathbf{y} = [y_1, \dots, y_{N_p}]^T$ is an indicator vector for popular contents, where y_l would be 1 if l^{th} content is stored in the cache of FAPs, otherwise it equals to 0. Similarly, $\mathbf{z} = [z_1, \dots, z_{N_a}]^T$ is an indicator variable for mediocre contents. According to the optimization problem, despite popular contents that are stored completely, just one segment of mediocre contents are cached. Similarly, y_l and z_l in constraint **C1** illustrate the availability of content c_l in the cache of FAP f_i . Finally, constraints **C2** and **C3** indicate the portion of cache allocated to popular and mediocre contents, respectively.

B. Content Placement in Multiple Inter-Clusters

After identifying popular and mediocre contents, we need to determine how to store different segments of mediocre contents within an inter-cluster. Lack of prior research studies on the coded content placement in a cluster-centric cellular network (e.g., [30], [31]) motivates us to propose the CCUF framework. Without loss of generality, we first consider a simple hexagonal cellular network including $N_s = 7$ FAPs as one inter-cluster (Fig. 3(a)). Given the vector $\mathbf{z} = [z_1, \dots, z_{N_a}]^T$ that determines the mediocre contents, in this phase, we need

to indicate which segment of the mediocre content c_l , denoted by c_{ls} for $(1 \leq l \leq N_a)$ and $(1 \leq s \leq N_s)$, should be cached in FAP f_i for $(1 \leq i \leq N_s)$. In this regard, we form an $N_a \times N_s$ indicator matrix of FAP f_i , denoted by \mathbf{Z}_{f_i} . Note that the l^{th} row of \mathbf{Z}_{f_i} indicates segments of file c_l is stored in the cache of FAP f_i , where $z_{ls} = 1$ means that s^{th} segment of file c_l is stored in the cache of FAP f_i . Consequently, the cached contents of other FAPs in an inter-cluster is determined as follows

$$z_{f_i, l} z_{f_j, l}^T = 0, \quad i = 1, \dots, N_s, j = 1, \dots, N_s, i \neq j, \quad (22)$$

where $z_{f_i, l}$ denotes the l^{th} row of \mathbf{Z}_{f_i} . After allocating mediocre contents to FAPs inside an inter-cluster, the same content as FAP f_i is stored in FAP f_k in the neighboring inter-cluster, where k is given by

$$\mathbf{Z}_{f_k} = \mathbf{Z}_{f_i} \quad \text{if} \quad k = w^2 + wz + z^2, \quad (23)$$

where w and z represent the number of FAPs required to reach another FAP storing similar contents, in two different directions. For example, in Fig. 3(a) $N_s = 7$, $w = 2$, and $z = 1$ for starting in a FAP including c_{15} and reaching the similar FAP in a neighboring inter-cluster. The main idea behind the coded placement scheme in our proposed CCUF framework comes from the frequency reusing technique in cellular networks [37]. In order to increase the resource availability and minimum inter-cell interference, the same radio frequencies are used in different cells, where the distance between two cells with the same spectrum bandwidth is determined based on Eq. (23).

Remark 1: As shown in Fig. 3(b), the coverage area of FAPs in a practical scenario is influenced by path loss and shadowing models. Location $p = (x, y)$ is placed within the transmission area of FAP f_i , if the strength of the received signal at point p , denoted by $RSSI_p$, is higher than the threshold value $RSSI_{th}$, where $RSSI_p$ is calculated as

$$RSSI_p(\text{dB}) = RSSI(d_0) + 10\eta \log_{10}\left(\frac{d}{d_0}\right) + X_\sigma, \quad (24)$$

where d and d_0 denote the distance between FAP and point p in the boundary of transmission area of FAP, and the reference distance is set to 1 m, respectively. Moreover, η represents the path loss exponent, which is 10 dB or 20 dB, and X_σ is a zero-mean Gaussian with standard deviation σ that represents the effect of multi-path fading in our UAV-based femtocaching scheme [38].

C. Cache-Hit Probability in the Proposed CCUF Framework

To quantify the benefits of the proposed CCUF strategy, we form the probability of finding a new segment by user GU_j at time slot t under the following two scenarios: (i) Uncoded cluster-centric, and; (ii) Coded cluster-centric UAV-aided femtocaching network, denoted by p_{uc} , and p_{cc} , respectively. Concerning the nature of mobile networks, ground users move and leave their current positions. In this paper, it is assumed that low-speed ground users can obtain one segment in each contact, i.e., $T = N_s \delta_t$ is required to completely download content c_l . First, we consider a simple mobility pattern, where ground users are positioned in the transmission

area of a new FAP in each time slot t . Eventually, in $T = N_s \delta_t$, the whole content c_l will be downloaded. Then, we generalize the mobility pattern to the DCRW model, where ground users are moving randomly.

1) *Simple Mobility Pattern*: Regarding the uncoded cluster-centric UAV aided femtocaching framework, content c_l consisting of c_{ls} , for $(1 \leq s \leq N_s)$ segments, is stored completely in all FAPs. Consequently, the probability of downloading $n = N_s$ segments of content c_l in $T = N_s \delta_t$ depends on the probability of requesting file c_l , denoted by p_l . Since the storage capacity of each FAP is equal to C_f , the cache-hit probability, denoted by p_{uc} , is obtained as follows

$$p_{uc}[n = N_s, t = T] = \sum_{l=1}^{C_f} p_l. \quad (25)$$

Note that, since contents are completely stored in uncoded cluster-centric framework, ground users can access the whole content in each contact. By considering the size of content and the speed of ground users, however, it is not possible to download more than one segment in each contact. Therefore, storing the whole of contents in all FAPs is not beneficial. On the other hand, the cache-hit probability in the coded cluster-centric UAV-aided femtocaching network is obtained as

$$p_{cc}[n = N_s, t = T] = \sum_{l=1}^{N_p} p_l + \sum_{l=N_p+1}^{N_s(C_f - \lfloor \alpha C_f \rfloor)} p_l. \quad (26)$$

To illustrate the growth rate of the cache-hit probability in the coded one, we rewrite p_{uc} in Eq. (25) as follows

$$p_{uc}[n = N_s, t = T] = \sum_{l=1}^{N_p} p_l + \sum_{l=N_p+1}^{C_f} p_l. \quad (27)$$

As it can be seen from Eqs. (26), and (27), the first term related to the popular content is the same. The second term, however, illustrates that the number of contents that can be served through FAPs in the coded cluster-centric network is \varkappa times greater than the uncoded one, where \varkappa is given by

$$\varkappa = \frac{N_s(C_f - \lfloor \alpha C_f \rfloor)}{C_f}. \quad (28)$$

Accordingly, due to the allocation of different segments in the coded cluster-centric network, more segments of the desired contents are accessible. Therefore, more requests can be served in comparison to the uncoded cluster-centric UAV-aided femtocaching networks.

2) *Generalizing to the DCRW Mobility Pattern*: Fig. 3(a) provides an overall overview of the proposed network, consisting of numerous inter-clusters, where ground users move randomly in all directions. In other words, it is possible for ground users to return back to the previous coverage area of FAPs (which is not considered in the simple mobility pattern). Moreover, in some cases, ground users may be positioned in the transmission area of a FAP, which stores the same segment of the required content that the ground user has already downloaded. Consequently, the cache-hit probability of the coded cluster-centric will not be the same as the previous scenario. If the requested content is the popular one, regardless

of the location of the ground user within an inter-cluster, the ground user can download one segment of the required content with the probability of $\sum_{l=1}^{N_p} p_l$ at each contact. Despite this part of the cache-hit probability, which is constant, the successful probability of downloading a new segment of a mediocre content in each contact depends on the current and all previous locations of the ground user. Therefore, we first determine the successful probability of achieving a new segment of a mediocre content, denoted by $p_{ns}(n = n_0, t = n_0 \delta_t)$, for $(1 \leq n_0 \leq N_s)$. Then, we calculate the cache-hit probability of a coded cluster-centric network based on the DCRW mobility pattern.

As it can be seen from Fig. 3(a), regardless of the location of GU_j , this user can download one segment successfully in the first contact (i.e., $n_0 = 1$). Therefore, we have $p_{ns}(n = 1, t = \delta_t) = 1$. Similarly, where $n_0 = 2$, the ground user GU_j can download a new segment without considering its location. Therefore, the probability of downloading two segments after two contacts is $p_{ns}[n = 2, t = 2\delta_t] = 1$. More precisely, in the second contact, the ground user can be positioned in the cell of $(N_s - 1)$ number of FAPs, where the probability of being in the cell of FAP f_i is $p(f = f_i) = \frac{1}{(N_s - 1)}$. Therefore, we have

$$\begin{aligned} p_{ns}[n = 2, t = 2\delta_t] &= \sum_{i=1}^{N_s-1} p_{ns}[n = 2, t = 2\delta_t | f = f_i] p(f = f_i) \\ &= (N_s - 1) \times 1 \times \frac{1}{(N_s - 1)} = 1. \end{aligned} \quad (29)$$

Accordingly, the probability of finding a new segment in the third contact is

$$\begin{aligned} p_{ns}[n = 3, t = 3\delta_t] &= \sum_{i=1}^{N_s-1} p_{ns}[n = 3, t = 3\delta_t | f = f_i] p(f = f_i) \\ &= (N_s - 2) \frac{1}{(N_s - 1)} \times 1 + \frac{1}{(N_s - 1)} \times 0 = \frac{(N_s - 2)}{(N_s - 1)}, \end{aligned} \quad (30)$$

where $(N_s - 2)$ FAPs have different segments, whereas if GU_j returns to the FAP at $t = \delta_t$, the ground user can find a similar segment. Considering the fact that $N_s = 7$ in our proposed wireless network, $p_{ns}[n = 3, t = 3\delta_t]$ would be 0.83. It means that user GU_j can find a new segment of the desired content in the third contact with a probability of 0.83. Similarly, it can be proved that the probability of finding a new segment in $n > 2$ is obtained as

$$\begin{aligned} p_{ns}[n = n_0, t = n_0 \delta_t] &= \sum_{i=1}^{N_s-1} p_{ns}[n = n_0, t = n_0 \delta_t | f = f_i] \\ &\times p(f = f_i) = \frac{(N_s - 2)^{n_0-2}}{(N_s - 1)^{n_0-2}}. \quad \text{for } n_0 > 2 \end{aligned} \quad (31)$$

Taking into account the unequal likelihood of finding new segments of mediocre contents in different contacts, we re-

Algorithm 1 Proposed CCUF Strategy

```

1: Initialization: Set  $\alpha$ ,  $\lambda$ ,  $N_s$ , and  $C_f$ .
2: Input:  $p_l^{(j)}(t)$ ,  $L_k^{(t)}$ , and  $L_j^{(t)}$ .
3: Output:  $x_l$ ,  $y_l$ , and  $z_l$ .
4: Content Placement Phase:
5: for  $u_k, k = 1, \dots, N_u$ , do
    
$$\min_{x_l} \sum_{l=1}^{N_c} \left( \sum_{j=1}^{N_g} (1 - p_l^{(j)}(t)) \mathcal{D}_u^{(j)}(t) \right) x_l$$

6:     s.t. C1. and C2. in Eq. (18).
7: end for
8: for  $f_i, i = 1, \dots, N_f$ , do
    
$$\min_{y_l, z_l} \sum_{l=1}^{\lfloor \alpha C_f \rfloor} \left( \sum_{j=1}^{N_g} (1 - p_l^{(j)}(t)) \mathcal{D}_f^{(j)}(t) \right) y_l +$$

    
$$\sum_{l=\lfloor \alpha C_f \rfloor + 1}^{N_s(C_f - \lfloor \alpha C_f \rfloor)} \left( \sum_{j=1}^{N_g} (1 - p_l^{(j)}(t)) \mathcal{D}_f^{(j)}(t) \right) z_l,$$

9:     s.t. C1. C3. in Eq. (21).
10: end for
11:  $z_{f_i, l} z_{f_j, l}^T = 0, \quad i = 1, \dots, N_s, j = 1, \dots, N_s, i \neq j,$ 
12:  $\mathbf{Z}_{f_k} = \mathbf{Z}_{f_i} \quad \text{if } k = w^2 + wz + z^2,$ 
13: Transmission Phase:
14: for  $GU_j, j = 1, \dots, N_g$ , do
15:     if  $GU_j$  is in indoor environment then
16:         if  $GU_j$  is an edge-user and requests
17:             popular content then
18:                 The request should be handled according to the
19:                 JT scheme.
20:             else
21:                 The request should be handled according to the
22:                 ST scheme.
23:             end if
24:         else
25:             if  $v_j(t) \geq v_{th}$  then
26:                 The request is served by UAV  $u_k$ .
27:             else
28:                 Similar to lines 16 to 23.
29:             end if
30:         end if
31:     end for
32: end for

```

calculate p_{cc} as follows

$$p_{cc}[n = N_s, t = T] = \sum_{l=1}^{N_p} p_l + \sum_{n=1}^{N_s} \frac{(N_s - 2)^{n-2}}{(N_s - 1)^{n-2}} \left(\sum_{l=N_p+1}^{N_s(C_f - \lfloor \alpha C_f \rfloor)} p_l \right). \quad (32)$$

D. 2-D Deployment of UAVs in Intra-clusters

To increase the resource availability for ground users, the outdoor environment is partitioned based on an unsupervised learning algorithm, each partition is covered by a UAV. Considering a Gaussian mixture distribution for ground users, we

have a dense population of ground users in some areas. The main goal is to deploy UAVs in such a way that ground users can experience high QoS communications even in a dense area. Note that the distance between UAVs and ground users is a critical factor that can significantly impact the QoS from different perspectives such as the energy consumption of UAVs and the users' access delay. Our goal is to partition N_g ground users into K intra-clusters, where the sum of Euclidean distances between the ground user GU_j , for $(1 \leq j \leq N_g^k)$, and UAV u_k is minimized. In this case, N_g^k is the cardinality of ground users positioned in the intra-cluster related to the UAV u_k . Therefore, the UAVs' deployment is obtained according to the following optimization problem

$$\min_{l_k(t)} \sum_{k=1}^{N_u} \sum_{j=1}^{N_g^k} \|l_j(t), l_k(t)\|, \quad (33)$$

where $l_k(t)$ denotes the location of the UAV u_k at time slot t , defined as the mean of the coordinates of all ground users inside the corresponding intra-cluster as follows

$$l_k(t) = \frac{\sum_{j=1}^{N_g^k} l_j(t)}{N_g^k}, \quad k = 1, \dots, N_u. \quad (34)$$

To solve the above optimization problem, we utilize the K-Means clustering algorithm [39], which is known as an efficient unsupervised learning framework. In the first step, a set of points, denoted by $\mathcal{P} = \{P_1, \dots, P_{N_u}\}$, is generated, where P_k for $(1 \leq k \leq N_u)$ should be within the pre-specified environment. Then, the set of ground users in the vicinity of P_k is determined as follows

$$u_j \in N_g^k \quad \text{if } \|l_j(t), P_k\| < \|l_j(t), P_r\|, \quad \forall k \neq r. \quad (35)$$

Given the set of ground users belonging to each intra-cluster, UAVs' locations are determined according to Eq. (34). In the second step, by moving ground users from one intra-cluster to another, the Euclidean distances between ground users and UAVs are calculated to update the location of UAVs according to Eq. (33). The K-Means algorithm is terminated when there is no change in the ground users belonging to an intra-cluster over several iterations. This completes our discussion on development of the CCUF scheme. The pseudo-code of the proposed CCUF framework is summarized in **Algorithm 1**.

IV. SIMULATION RESULTS

To demonstrate the advantage of the proposed CCUF framework, we consider a macro cellular network consisting of one MBS with the radius $R = 1000$ m, $N_f = 180$ FAPs, and $N_u = 10$ UAVs, where each inter-cluster comprises of $N_s = 7$ FAPs. Fig. 4 illustrates a typical 20×20 m^2 area, where ground users are randomly distributed and their locations are determined according to the AoA localization method. It can be shown that the Root Mean Square Error (RMSE) between the estimated and the actual location of the ground users is about 0.4 m, which is acceptable in comparison to the transmission range of FAPs.

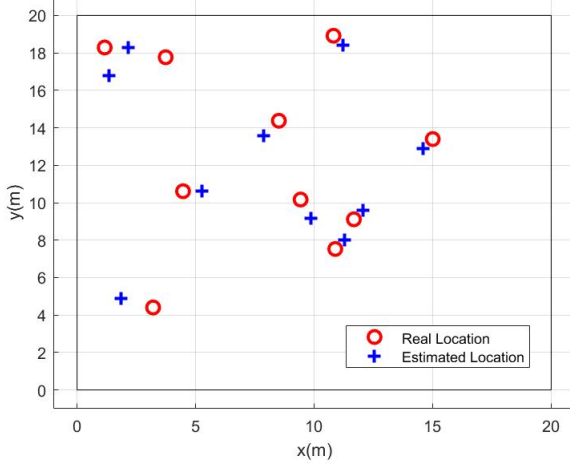


Fig. 4: Typical location estimation results based on the AoA localization scheme.

Fig. 5 depicts an integrated heterogeneous network, where yellow and red areas determine indoor and outdoor environments, respectively. Fig. 5 also shows the deployment of UAVs in the intra-clusters within the network, which is generated by partitioning ground users according to the K-means clustering algorithm. As a result of the Gaussian mixture distribution for clients, we have a dense population in some areas, which can be changed over time by the movement of ground users. Therefore, the location of $N_u = 10$ UAVs and the formation of intra-clusters in this paper is varying, depending on the user density distribution. The general simulation parameters are summarized in Table I. In order to find the optimum value of α , three types of caching strategies are considered:

- *Uncoded UAV-aided Femtocaching (UUF)*: Without coding and clustering, popular contents are stored completely into FAPs and UAVs. In this case, the value of α , which indicates the percentage of contents stored completely, would be one (i.e., $\alpha = 1$).
- *Proposed Cluster-centric and Coded UAV-aided Femtocaching (CCUF)*: In this case, the uncoded popular and the coded mediocre contents are stored in the caching nodes, where $0 < \alpha < 1$. According to the simulation results, the best value of α is obtained.
- *The Conventional Cluster-centric and Coded UAV-aided Femtocaching (Conventional CCUF)*: In this framework, regardless of the content popularity profile, all contents are stored partially in this framework. Consequently, the value of α is equal to zero.

These three strategies are evaluated over the cache-hit-ratio, cache diversity, cache redundancy, SINR, and users' access delay to determine the best value of α . Moreover, to illustrate the effect of considering a UAV-aided femtocaching framework in an integrated network, we compare the users' access delay and energy consumption of UAVs, by serving users in both indoor and outdoor areas.

Cache-Hit-Ratio: This metric illustrates the number of requests served by caching nodes versus the total number of requests made across the network. The high value of cache-hit-ratio shows the superiority of the framework. Since we assume

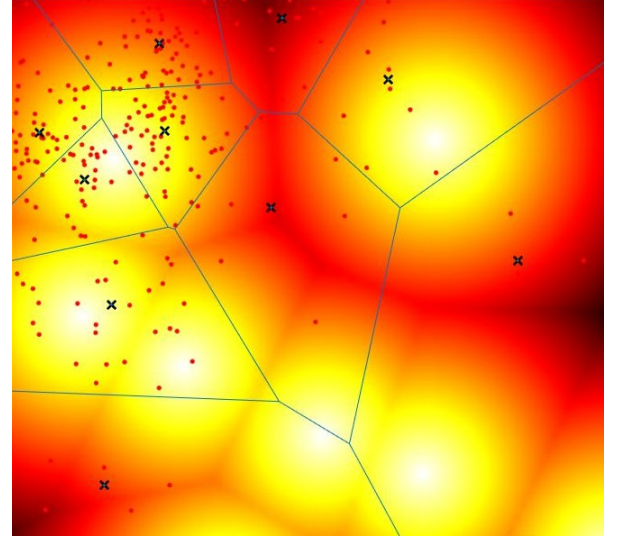


Fig. 5: Deployment of UAVs in intra-clusters within an integrated network, where "yellow" and "red" colors indicate indoor and outdoor environments, respectively.

TABLE I: List of Parameters.

Notation	Value	Notation	Value
N_g	500	$\eta^{(LoS)}, \eta^{(NLoS)}$	1.2, 3
N_f	180	h_k	100 m
N_u	10	ϖ, ψ	2, 20
N_s	7	L_c	37.5 MB
N_c	40724	τ_p	0 – 5 s
R_u	250 m	P_k	15 dBm
R_f	30 m	$\chi_\sigma^{(LoS)}, \chi_\sigma^{(NLoS)}$	3.5, 3
$P_T(t), P_R(t)$	0.5, 0.25 W	N_0	-94 dBm

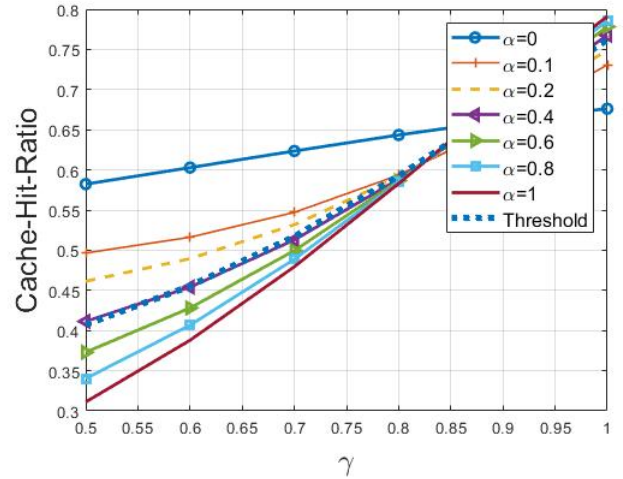


Fig. 6: The cache-hit-ratio versus the popularity parameter γ for different values of α . that ground users can download one segment in each contact, we evaluate the cache-hit-ratio in terms of the number of fragmented contents served by caching nodes. Fig. 6 compares the cache-hit-ratio of the UUF ($\alpha = 1$), the proposed CCUF ($0 < \alpha < 1$), and conventional CCUF ($\alpha = 0$) frameworks versus the value of γ . As previously mentioned, parameter γ shows the skewness of the content popularity, where $\gamma \in [0, 1]$. Note that the large value of γ indicates that a small number of contents has a high popularity, where a small value of

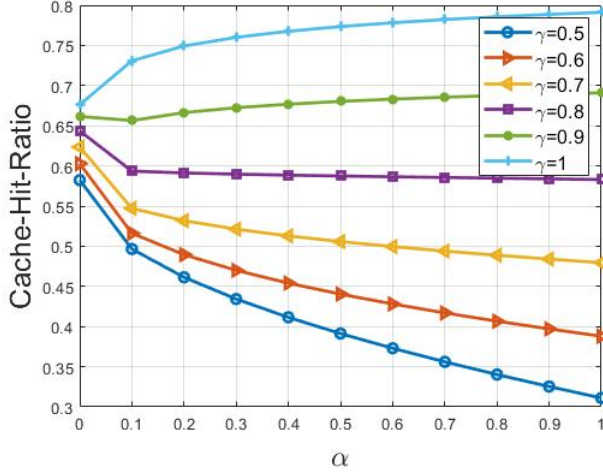


Fig. 7: The cache-hit-ratio versus the α percentage of contents that are stored completely.

γ illustrates an almost uniform popularity distribution for the majority of contents. As it can be seen from Fig. 6, depending on the popularity distribution of contents, γ , the conventional CCUF framework results in a higher cache-hit-ratio. The most important reason is that given a constant cache capacity, the coded content placement of the conventional CCUF strategy leads to a remarkable surge in the content diversity. In contrast, for a high value of γ , where a small number of contents is widely requested, the UUF and the proposed CCUF frameworks have better results compared to the conventional CCUF. By considering the fact that the common value of γ is about $0.5 \leq \gamma \leq 0.6$ (e.g., see [4], [29], [40]), we define CHR_{th} as the threshold cache-hit-ratio, which is the average of cache-hit-ratio of different values of α for a specific γ . As it can be seen from Fig. 6, the proposed CCUF framework with $0 < \alpha \leq 0.4$ and the UUF scheme outperform other schemes from the aspect of cache-hit-ratio.

Fig. 7 shows the cache-hit-ratio versus different values of α when the popularity parameter γ changes in the range of 0.5 to 1. Accordingly, for $0.5 \leq \gamma \leq 0.6$, by increasing the value of α , the cache-hit-ratio decreases drastically. In the following, we also investigate the impact of α on the users' access delay to determine the best value of α .

Users' Access Delay: Users' access delay depends on three parameters, i.e., the availability of the content in caching nodes, the distance between the ground user and the corresponding caching node, and the channel quality, known as the SINR. Figs. 8 and 9 compare the users' access delay of the aforementioned frameworks, which is obtained according to Eq. (19). By utilizing the CoMP technology in the proposed CCUF, serving edge-users according to the JT scheme has a great impact on the SINR, where users' access delay decrease by increasing the SINR. As can be seen from Table II, the SINR of edge-users improves by increasing the value of α . Note that JT scheme can be performed if the same contents are stored in the neighboring FAPs. Therefore, by increasing the value of α , the users' access delay will decrease. With the same argument, we define \mathcal{D}_{th} , which is the average of users' access delay of different values of α for a specific γ ,

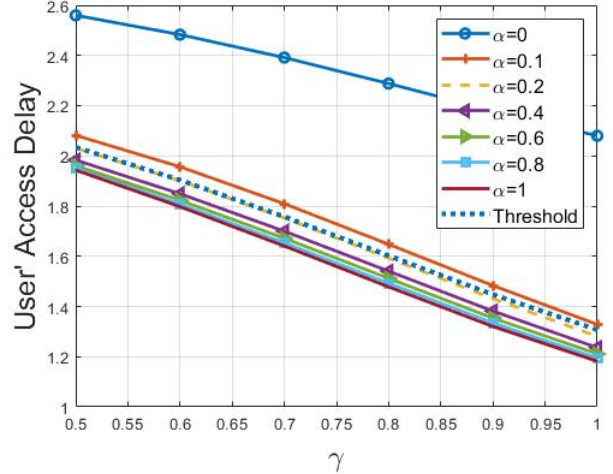


Fig. 8: The users' access delay in the indoor environment versus different value of γ .

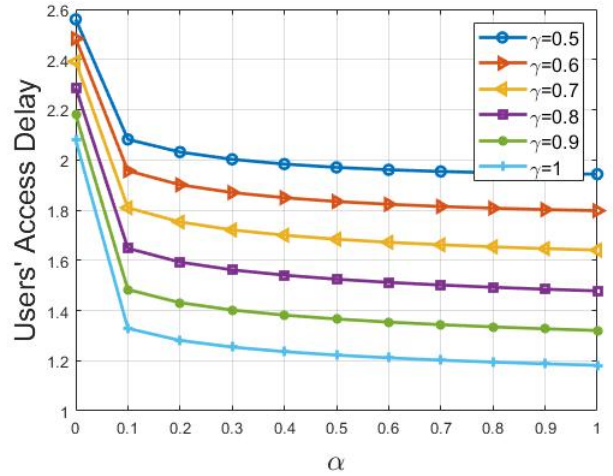


Fig. 9: The users' access delay in the indoor environment versus different values of α .

TABLE II: The SINR experienced by edge-users for different values of α and γ .

	$\gamma = 0.5$	$\gamma = 0.6$	$\gamma = 0.7$	$\gamma = 0.8$	$\gamma = 0.9$	$\gamma = 1$
$\alpha = 0$	16.37	16.37	16.37	16.37	16.37	16.37
$\alpha = 0.1$	17.55	18.12	18.89	19.84	20.88	21.88
$\alpha = 0.2$	18.01	18.65	19.46	20.40	21.38	22.30
$\alpha = 0.4$	18.62	19.30	20.11	21.00	21.90	22.70
$\alpha = 0.6$	19.06	19.75	20.53	21.37	22.20	22.93
$\alpha = 0.8$	19.42	20.09	20.85	21.64	22.42	23.08
$\alpha = 1$	19.72	20.38	21.11	21.86	22.58	23.20

shown in Fig. 8. Therefore, the best value of α would be $\alpha \geq 0.2$. Consequently, the cache-hit-ratio and users' access delay of the proposed CCUF framework would be efficient if $\alpha \in [0.2, 0.4]$.

Cache Diversity: This metric illustrates the diversity of contents in an inter-cluster, which is defined as the number of distinct segments of contents, expressed as follows

$$CD = \frac{N_a}{N_s C_f} = 1 - \frac{[\alpha C_f]}{C_f}. \quad (36)$$

As stated previously, we have $N_a = N_s(C_f - [\alpha C_f])$. As it can be seen from Fig. 10, the value of CD would be one,

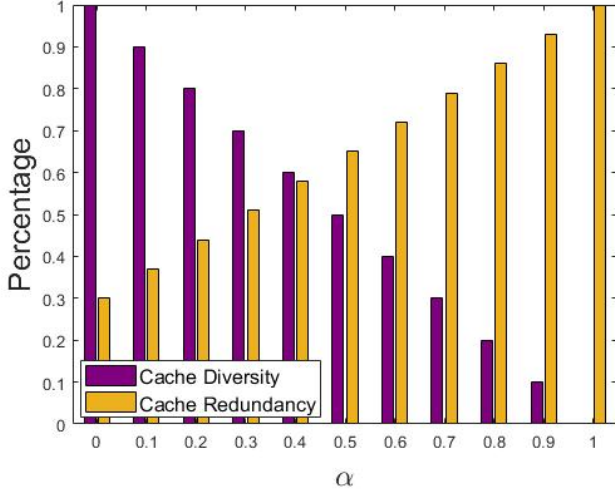


Fig. 10: The percentage of the cache diversity and the cache redundancy versus different values of α .

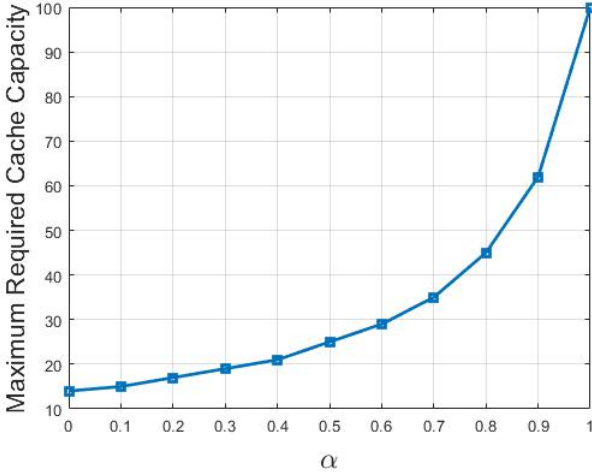


Fig. 11: The maximum cache capacity, required to achieve the maximum cache diversity, versus different values of α .

if $\alpha = 0$, which means that all cached contents are different. The cache diversity, however, linearly decreases by increasing the value of α , and reaches the lowest value zero, when all contents are cached completely (i.e., $\alpha = 1$).

Cache Redundancy: This metric indicates the number of similar contents that ground users meet during their random movements. As it can be seen from Fig. 10, the cache redundancy increases by storing the entire contents. By considering the coded content placement, even in the proposed CCUF framework, ground users that move randomly through the network, can meet a similar coded contents during their movements (see Fig. 3).

Maximum Required Cache Capacity: Given a specific number of contents through the network, denoted by N_c , the storage capacity of caching nodes is determined by $C_f = \beta N_c$. In this case, parameter β indicates the percentage of contents that can be stored in caching nodes. In the coded content placement, since only one segment of the contents is cached, it is fairly likely that the total number of possible segments that can

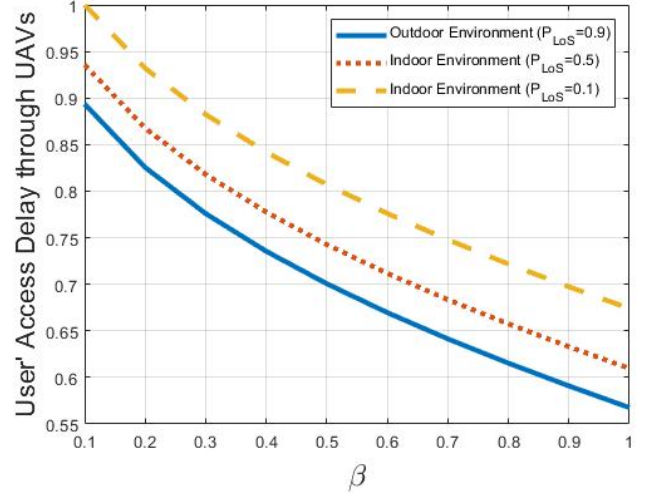


Fig. 12: The users' access delay experienced through UAVs in both indoor and outdoor versus different values of β .

be cached exceeds the total number of contents. Therefore, the maximum required cache capacity, denoted by β_{max} , for different values of α is obtained as

$$\beta_{max} \leq \frac{N_c}{N_s N_c - (N_s - 1) \alpha N_c} = \frac{1}{\alpha(1 - N_s) + N_s}, \quad (37)$$

where the remainder of the storage would be occupied by redundant contents if $\beta > \beta_{max}$. As it can be seen from Fig. 11, the maximum cache capacity β_{max} increases by the value of α . Consequently, in smaller values of α , we need a smaller cache capacity to have the maximum cache diversity.

Users' Access Delay through UAVs and UAVs' Energy Consumption: Finally, we evaluate the users' access delay and the energy consumption of UAVs in Figs. 12 and 13, when the corresponding ground user is located in both indoor and outdoor environments. According to Eqs. (11), and (16), and (17), the probability of establishing a LoS connection between the ground user GU_j and the UAV u_k has a great impact on the users' access delay, served by UAVs. To tackle this problem, we assume that ground users in indoor areas are served by inter-clusters. With the same argument, Fig. 13 illustrates the energy consumption of UAVs, calculated as follows [8]

$$E_{u_k}^{(LoS)}(t) = L_c P_T(t) \tau_p + L_c P_R(t) \tau_p + P_j^{(LoS)}(t) (\tau_f - \tau_p), \quad (38)$$

$$E_{u_k}^{(NLoS)}(t) = L_c P_T(t) \tau_p + L_c P_R(t) \tau_p + P_j^{(NLoS)}(t) (\tau_f - \tau_p), \quad (39)$$

where $P_T(t)$ and $P_R(t)$ represent the power consumed for transmission and reception powers of 1 Mb file, respectively. Moreover, $P_j(t)$, τ_f , and τ_p denote the received power at ground user GU_j , and the flyby and the pause times of UAV u_k , respectively.

V. CONCLUSIONS

In this paper, we developed a Cluster-centric and Coded UAV-aided Femtocaching (CCUF) framework for an integrated and dynamic cellular network to maximize the number of requests served by caching nodes. To increase the cache

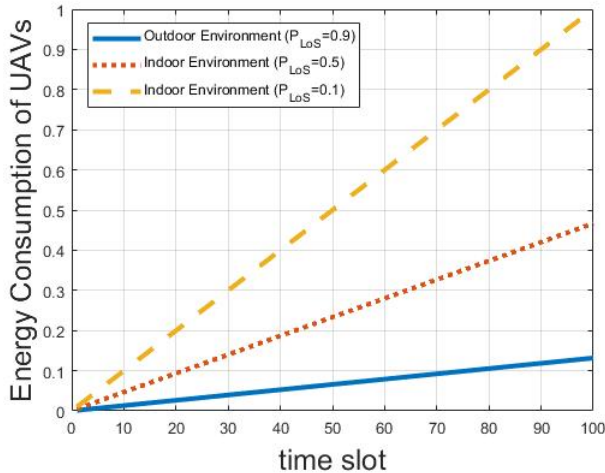


Fig. 13: The energy consumption of UAVs in both indoor and outdoor environments in different time slots.

diversity and to store distinct segments of contents in neighboring FAPs, we employed a two-phase clustering technique for FAPs' formation and UAVs' deployment. In this case, we analytically formulated the cache-hit probability of the proposed CCUF framework. Moreover, in the cluster-centric cellular network, multimedia contents were coded based on their popularity profiles. In order to benefit the Coordinated Multi-Point (CoMP) technology and to improve the inter-cell interference, we determined the best value of the number of contents that should be stored completely. According to the simulation results and by considering the optimum value of α , the proposed CCUF framework results in an increase in the cache-hit-ratio, SINR, and cache diversity and decrease users' access delay and cache redundancy. Going forward, several directions deserve further investigation. First, it is of interest to introduce a Reinforcement Learning (RL)-based method for outdoor environment, where ground users can be autonomously served by UAVs or FAPs, based on the dynamic population of their current locations and their speeds. Second, the optimum number of ground users to be served by a UAV in the proposed network needs to be analyzed.

REFERENCES

- [1] V. Chamola, V. Hassija, V. Gupta and M. Guizani, "A Comprehensive Review of the COVID-19 Pandemic and the Role of IoT, Drones, AI, Blockchain, and 5G in Managing its Impact," *IEEE Access*, vol. 8, pp. 90225-90265, May 2020.
- [2] H. Hui, Y. Ding, Q. Shi, F. Li, Y. Song, and J. Yan, "5G network-based Internet of Things for Demand Response in Smart Grid: A survey on Application Potential," *Applied Energy*, vol. 257, pp. 113972-113987, Jan. 2020.
- [3] Z. Hajiakhondi-Meybodi, J. Abouei, and A. H. F. Raouf, "Cache Replacement Schemes Based on Adaptive Time Window for Video on Demand Services in Femtocell Networks," *IEEE Transactions on Mobile Computing*, vol. 18, no. 7, pp. 1476-1487, July 2019.
- [4] Z. Hajiakhondi-Meybodi, J. Abouei, M. Jaseemuddin and A. Mohammadi, "Mobility-Aware Femtocaching Algorithm in D2D Networks Based on Handover," accepted for publication in *IEEE Transactions on Vehicular Technology*, June 2020.
- [5] B. Jiang, J. Yang, H. Xu, H. Song, and G. Zheng, "Multimedia Data Throughput Maximization in Internet-of-Things System Based on Optimization of Cache-Enabled UAV," *IEEE Internet of Things Journal*, vol. 6, no. 2, pp. 3525-3532, Apr. 2019.
- [6] F. Cheng, G. Gui, N. Zhao, Y. Chen, J. Tang, and H. Sari, "UAV-Relaying-Assisted Secure Transmission With Caching," *IEEE Transactions on Communications*, vol. 67, no. 5, pp. 3140-3153, May 2019.
- [7] N. Zhao, F. Cheng, F. R. Yu, J. Tang, Y. Chen, G. Gui, and H. Sari, "Caching UAV Assisted Secure Transmission in Hyper-Dense Networks Based on Interference Alignment," *IEEE Transactions on Communications*, vol. 66, no. 5, pp. 2281-2294, May 2018.
- [8] V. Sharma, I. You, D. N. K. Jayakody, D. G. Reina, and K. K. R. Choo, "Neural-Blockchain-Based Ultrareliable Caching for Edge-Enabled UAV Networks," *IEEE Transactions on Industrial Informatics*, vol. 15, no. 10, pp. 5723-5736, Oct. 2019.
- [9] J. Lee, K. Kim, M. Kim, J. Park, Y. K. Yoon and Y. J. Chong, "Measurement-Based Millimeter-Wave Angular and Delay Dispersion Characteristics of Outdoor-to-Indoor Propagation for 5G Millimeter-Wave Systems," *IEEE Access*, vol. 7, pp. 150492-150504, Oct. 2019.
- [10] R. Avanzato and F. Beritelli, "A Smart UAV-Femtocell Data Sensing System for Post-Earthquake Localization of People," *IEEE Access*, vol. 8, pp. 30262-30270, Feb. 2020.
- [11] Z. Wang, L. Duan and R. Zhang, "Adaptive Deployment for UAV-Aided Communication Networks," *IEEE Transactions on Wireless Communications*, vol. 18, no. 9, pp. 4531-4543, Sept. 2019.
- [12] X. Liu, Y. Liu and Y. Chen, "Reinforcement Learning in Multiple-UAV Networks: Deployment and Movement Design," *IEEE Transactions on Vehicular Technology*, vol. 68, no. 8, pp. 8036-8049, Aug. 2019.
- [13] M. Samir, S. Sharafeddine, C. Assi, T. M. Nguyen, and A. Ghayeb, "Trajectory Planning and Resource Allocation of Multiple UAVs for Data Delivery in Vehicular Networks," *IEEE Networking Letters*, vol. 1, no. 3, pp. 107-110, Sept. 2019.
- [14] S. Li, B. Duo, X. Yuan, Y. Liang and M. Di Renzo, "Reconfigurable Intelligent Surface Assisted UAV Communication: Joint Trajectory Design and Passive Beamforming," *IEEE Wireless Communications Letters*, vol. 9, no. 5, pp. 716-720, May 2020.
- [15] M. Chen, W. Saad, and C. Yin, "Liquid State Machine Learning for Resource and Cache Management in LTE-U Unmanned Aerial Vehicle (UAV) Networks," *IEEE Transactions on Wireless Communications*, vol. 18, no. 3, pp. 1504-1517, Mar. 2019.
- [16] Z. Yang, C. Pan, K. Wang and M. Shikh-Bahaei, "Energy Efficient Resource Allocation in UAV-Enabled Mobile Edge Computing Networks," *IEEE Transactions on Wireless Communications*, vol. 18, no. 9, pp. 4576-4589, Sept. 2019.
- [17] B. Ji, Y. Li, B. Zhou, C. Li, K. Song, and H. Wen, "Performance Analysis of UAV Relay Assisted IoT Communication Network Enhanced With Energy Harvesting," *IEEE Access*, vol. 7, pp. 38738-38747, Mar. 2019.
- [18] L. Zhang, Z. Zhao, Q. Wu, H. Zhao, H. Xu, and X. Wu, "Energy-Aware Dynamic Resource Allocation in UAV Assisted Mobile Edge Computing Over Social Internet of Vehicles," *IEEE Access*, vol. 6, pp. 56700-56715, Oct. 2018.
- [19] B. Li, Z. Fei, and Y. Zhang, "UAV Communications for 5G and Beyond: Recent Advances and Future Trends," *IEEE Internet of Things Journal*, vol. 6, no. 2, pp. 2241-2263, Apr. 2019.
- [20] M. Chen, W. Saad, and C. Yin, "Echo-Liquid State Deep Learning for 360 Content Transmission and Caching in Wireless VR Networks With Cellular-Connected UAVs," *IEEE Transactions on Communications*, vol. 67, no. 9, pp. 6386-6400, Sept. 2019.
- [21] H. Wu, X. Tao, N. Zhang, and X. Shen, "Cooperative UAV Cluster-Assisted Terrestrial Cellular Networks for Ubiquitous Coverage," *IEEE Journal on Selected Areas in Communications*, vol. 36, no. 9, pp. 2045-2058, Sept. 2018.
- [22] M. Chen, M. Mozaffari, W. Saad, C. Yin, M. Debbah, and C. S. Hong, "Caching in the Sky: Proactive Deployment of Cache-Enabled Unmanned Aerial Vehicles for Optimized Quality-of-Experience," *IEEE Journal on Selected Areas in Communications*, vol. 35, no. 5, pp. 1046-1061, May 2017.
- [23] S. Suman, S. Kumar and S. De, "Path Loss Model for UAV-Assisted RFET," *IEEE Communications Letters*, vol. 22, no. 10, pp. 2048-2051, Oct. 2018.
- [24] Z. Hu, Z. Zheng, L. Song, T. Wang and X. Li, "UAV Offloading: Spectrum Trading Contract Design for UAV-Assisted Cellular Networks," *IEEE Transactions on Wireless Communications*, vol. 17, no. 9, pp. 6093-6107, Sept. 2018.
- [25] D. Athukoralage, I. Guvenc, W. Saad and M. Bennis, "Regret Based Learning for UAV Assisted LTE-U/WiFi Public Safety Networks," *IEEE Global Communications Conference (GLOBECOM)*, Washington, Feb. 2017 pp. 1-7.

- [26] S. Zhu, L. Gui, N. Cheng, F. Sun and Q. Zhang, "Joint Design of Access Point Selection and Path Planning for UAV-Assisted Cellular Networks," *IEEE Internet of Things Journal*, vol. 7, no. 1, pp. 220-233, Jan. 2020.
- [27] E. Recayte, F. Lazaro, and G. Liva, "Caching at the Edge with Fountain Codes," in *Proc. Advanced Satellite Multimedia Systems Conference and the Signal Processing for Space Communications Workshop (ASMS/SPSC)*, Berlin, Oct. 2018, pp. 1-6.
- [28] D. Ko, B. Hong, and W. Choi, "Probabilistic Caching Based on Maximum Distance Separable Code in a User-Centric Clustered Cache-Aided Wireless Network," *IEEE Transactions on Wireless Communications*, vol. 18, no. 3, pp. 1792-1804, Mar. 2019.
- [29] K. Shanmugam, N. Golrezaei, A. G. Dimakis, A. F. Molisch and G. Caire, "FemtoCaching: Wireless Content Delivery Through Distributed Caching Helpers," *IEEE Transactions on Information Theory*, vol. 59, no. 12, pp. 8402-8413, Dec. 2013.
- [30] D. Ren, X. Gui, K. Zhang, and J. Wu, J., "Hybrid Collaborative Caching in Mobile Edge Networks: An Analytical Approach," *Computer Networks*, vol. 158, pp.1-16, July 2019.
- [31] Z. Chen, J. Lee, T. Q. S. Quek and M. Kountouris, "Cooperative Caching and Transmission Design in Cluster-Centric Small Cell Networks," *IEEE Transactions on Wireless Communications*, vol. 16, no. 5, pp. 3401-3415, May 2017.
- [32] P. Lin, Q. Song, J. Song, A. Jamalipour and F. R. Yu, "Cooperative Caching and Transmission in CoMP-Integrated Cellular Networks Using Reinforcement Learning," *IEEE Transactions on Vehicular Technology*, vol. 69, no. 5, pp. 5508-5520, May 2020.
- [33] Z. HajiAkhondi-Meybodi, M. S. Beni, K. N. Plataniotis, and A. Mohammadi "Bluetooth Low Energy-based Angle of Arrival Estimation via Switch Antenna Array for Indoor Localization," *International Conference on Information Fusion*, July 2020.
- [34] Z. HajiAkhondi-Meybodi, M. S. Beni, A. Mohammadi, and K. N. Plataniotis, "Bluetooth Low Energy-based Angle of Arrival Estimation in Presence of Rayleigh Fading," Accepted in *IEEE International Conference on Systems, Man, and Cybernetics*, 2020.
- [35] C. M. Albertsen, "Generalizing the First-Difference Correlated Random Walk for Marine Animal Movement Data," *Scientific Reports*, vol. 9, no. 1, pp. 4017-4031, Mar. 2019.
- [36] L. Qiu and G. Cao, "Popularity-Aware Caching Increases the Capacity of Wireless Networks," *IEEE Transactions on Mobile Computing*, vol.19, no. 1, pp. 173-87, Jan. 2019.
- [37] Y. Choi, C. S. Kim and S. Bahk, "Flexible Design of Frequency Reuse Factor in OFDMA Cellular Networks," *IEEE International Conference on Communications*, Istanbul, 2006, pp. 1784-1788.
- [38] A. M. Al-Samman, T. A. Rahman, T. Al-Hadhrani, A. Daho, M. N. Hindia, M. H. Azmi, K. Dimiyati, and M. Alazab, "Comparative Study of Indoor Propagation Model Below and Above 6 GHz for 5G Wireless Networks," *Electronics*, vol. 18, no. 1, Jan. 2019.
- [39] T. Kanungo, D. M. Mount, N. S. Netanyahu, C. D. Piatko, R. Silverman and A. Y. Wu, "An efficient k-means clustering algorithm: analysis and implementation," *IEEE Transactions on Pattern Analysis and Machine Intelligence*, vol. 24, no. 7, pp. 881-892, July 2002.
- [40] T. Zhang, Y. Wang, Y. Liu, W. Xu and A. Nallanathan, "Cache-enabling UAV Communications: Network Deployment and Resource Allocation," *IEEE Transactions on Wireless Communications*, July 2020.